J. Fluid Mech. (1972), *vol.* 53, *part* 4, *pp.* 593–610
Printed in Great Britain

An experimental investigation of an asymmetrical turbulent wake

By M. D. PALMER† AND J. F. KEFFER
Department of Mechanical Engineering, University of Toronto

(Received 8 November 1971)

Experiments on the two-dimensional turbulent wake generated by pairs of cylinders of unequal diameter have revealed some interesting flow characteristics. The wake width grew asymmetrically in the downstream direction, spread rate and entrainment coefficients proving larger on the small diameter cylinder side. Mean velocity profiles were also skewed to this side while maximum values of Reynolds stresses were larger on the other. Close to the cylinder, a region or turbulent 'energy reversal' was measured. The level of turbulence and the diffusion mechanism were high at this point and some comments are made concerning the structure of the flow under these conditions.

1. Introduction

Almost all our present understanding of the mechanics of turbulent shear flows has been obtained from experimental studies. Not surprisingly, the most commonly examined flow fields have been symmetric, such as jets and wakes, or those with monotonic mean velocity gradients as in mixing layers and boundary layers. For these situations a reasonable knowledge of the mean and turbulent flow characteristics has been accumulated (Townsend 1956; Schlichting 1968).

However, in those relatively few cases where an essential asymmetry of the mean velocity profile exists, some unexpected features of the flow have emerged. For example, in the two-dimensional wall jet formed by a stream blown tangentially along a fixed boundary, the fully developed mean velocity profile is double-structured, resembling a flat-plate boundary layer near the wall and a free-jet profile in the outer region. Kruka & Eskinazi (1964) and Béguier (1965) observed a non-coincidence between the point of maximum mean velocity and the position of zero turbulent shear stress for this flow. This is rather unusual. Generally, we consider that mean flow kinetic energy is converted to turbulent kinetic energy through the interaction of the turbulent Reynolds stresses with the mean velocity gradient. This process is called turbulent kinetic energy production and for symmetric flows always gives an increase in energy as any changes in sign of $\overline{uv}$ and dU/dy occur together. Furthermore, the presence of viscosity in the fluid ensures an eventual transfer of the kinetic energy to successively higher wavenumbers in the spectral regime until it is finally dissipated

† Present address: Ontario Water Resources Commission, Toronto.

as heat in the very smallest eddies. Clearly, the direction of transport of energy must be from the mean motion to the highest wavenumbers of the turbulent flow.

In the wall jet, however, the non-coincidence results in the turbulent energy production term becoming negative over a measurable region of the flow. It is of interest that a similar effect has been observed more recently by Wong & Brundidge (1966) and by Deissler (1968) in atmospheric situations. Although the overall direction of the transfer of turbulent kinetic energy is prescribed by external conditions there appears to be no valid reason why these local reversals cannot take place. In fact, Lumley & Panofsky (1964) have suggested renaming the process 'energy feeding' since it can take any sign locally. The aim of the present investigation was to create a significantly large region on a laboratory scale in which this phenomenon could be observed.

2. Experimental method

2.1. *The wake flow*

Because of the large amount of well-documented literature on the two-dimensional turbulent wake, attempts were made to generate the asymmetry by a parallel cylinder configuration. It has been shown for a single circular cylinder that the motion beyond about 200 diameters is essentially self-preserving, the velocity and length scales having a predictable functional dependence upon the streamwise co-ordinate (Townsend 1956). Closer than this, from approximately 50–200 diameters, the mean quantities are self-similar only if profiles are stretched by local velocity and length scales (Alexopoulos & Keffer 1968). Comparatively less is known about the region immediately downstream from the cylinder. Kuethe (1951), Bloor (1964), Gerrard (1965) and Hama (1962) have examined the flow within the first few diameters but the investigations have been directed more towards the development of the mean flow characteristics than consideration of the details of the kinetic energy content. A quantitative description of the wake within the development region, however, is difficult to obtain since the velocity field immediately downstream of the cylinder is intermittent – a result of the strong vortex action. We thus restricted measurements to the region more than 14 diameters from the cylinder.

2.2. *Asymmetry*

Several different methods for generating the asymmetry were tried. In each case flow visualization techniques were employed as a preliminary check on the structure of the wake. It was eventually decided to use pairs of cylinders with unequal diameters, these configurations having shown a strong asymmetric vortex formation in the immediate wake which persisted for a considerable distance downstream. Additional tests suggested that a gap spacing for the cylinder pair of the order of the cylinder diameters would be most effective. The work of Spivack (1946) had given some indication as to the best choice of differential size for the pair and gap.

The specific configurations used are listed in table 1. The sequence of numbers denotes in mm the upper cylinder diameter, the gap size and the lower cylinder

Configuration	Total diameter D (mm)	x/D	Third moment (skewness)	Half-wake width: Small cylinder D	Half-wake width: Large cylinder D
12·7, 6·35, 12·7	31·75	14·6	−0·00462	0·80	0·80
		80·0	−0·00299	2·4	2·5
12·7, 6·35, 15·9	34·95	14·6	−0·044	0·88	0·66
		80·0	−0·0105	3·2	2·5
9·52, 4·78, 15·9	30·20	14·6	−0·0397	0·76	0·60
		80·0	−0·0245	2·5	2·0
9·52, 6·35, 15·9	31·77	14·6	−0·0220	0·98	0·73
		80·0	−0·0141	2·5	2·1
Townsend (1956)		80·0	0·00	2·5	2·5

TABLE 1. Asymmetry characteristics of mean velocity profiles

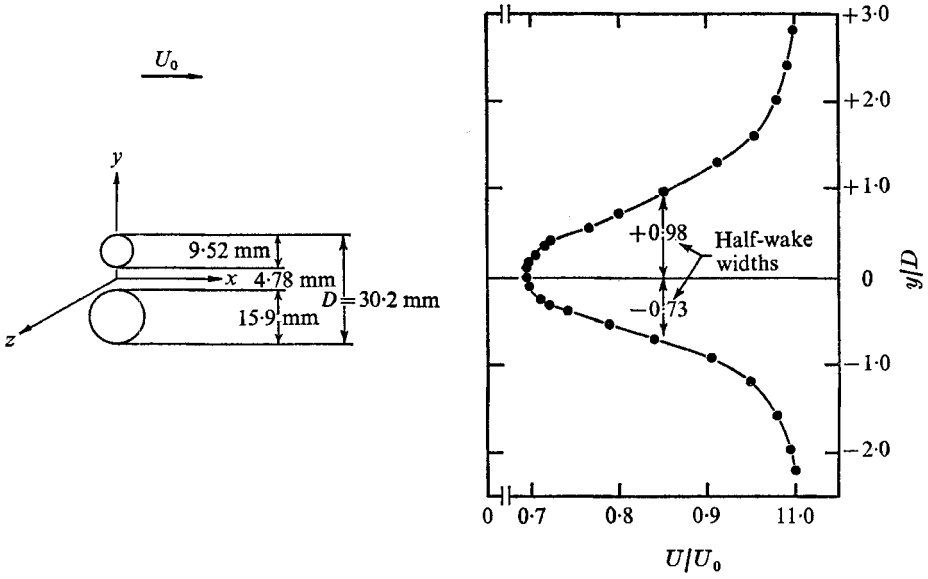

FIGURE 1. Definition sketch for asymmetric cylinder pair (9·52, 6·35, 15·9); $y = 0$ is defined as the maximum defect velocity point.

diameter respectively. A typical example is shown in figure 1 for the configuration (9·52, 4·78, 15·9). A symmetrical pair and was used as a control for the other three asymmetric combinations. The effective diameter D was defined as the diameter of each cylinder plus the gap width and was kept roughly constant for each pair. An alternative choice is the single cylinder diameter required to produce the drag for the cylinder pair. Integration of the mean velocity defects at $x/D = 80$, the limit of the test section, showed these values to be almost identical, and for convenience D was used to non-dimensionalize all lengths.

The configurations were tested in the UTME Low Turbulence Wind Tunnel.

A free-stream velocity of 4 ms^{-1} was selected for the tests. This was the smallest value which gave a flow Reynolds number ($Re = U_0 D/\nu$) not less than 5000. The free-stream turbulence level at this tunnel speed was $(\overline{u^2})^{\frac{1}{2}}/U = 0{\cdot}0004$. The turbulence characteristics were measured with linearized hot-wire anemometer equipment (Disa CTA 55D01 and Linearizer Model 55D10) and the usual supporting instrumentation such as an oscilloscope, random-signal voltmeter and spectrum analyser. A co-ordinate system was selected with the x direction along the axis of the composite wake and the y and z directions, the normal and binormal to x, as shown in the definition sketch, figure 1. The origin for the y co-ordinate was taken as the minimum mean velocity point in the composite wake, i.e. the position of the maximum velocity defect. The sensors were positioned within the tunnel via a remote-control servo-traversing carriage. This was capable of fixing a probe in the y, z plane to within 0·02 mm and to within 3·0 mm in the streamwise direction.

2.3. *Experimental programme*

The individual cylinder length-to-diameter ratio was approximately 60. Each end was threaded for mounting in a tensioning rack which in turn was fixed firmly to the walls of the test section, which were 0·9 m apart. Precisely machined spacers were used at the quarter points to set the gap spacing. As a check, a series of tests was run to determine the effect of permissible misalignment upon the evaluation of the mean flow. Any such error was within the limits of the measurement accuracy and could be ignored.

The lateral Reynolds stresses $\overline{uw}$ were measured for the cylinder pairs and found to be negligibly small. On this basis it was assumed that the flows were essentially two-dimensional.

Wake widths were defined in the conventional manner as the distance (y direction) between the 'half-velocity' points on the mean profiles. 'Half-velocity' was taken as the mean of the free-stream velocity and the minimum mean velocity at any cross-section downstream of the cylinders, i.e. $\frac{1}{2}(U_0 + U_m)$. For the twin-cylinder wakes the width was expressed as the sum of the two components referred to as 'half-wake' widths. For example, the wake width for the configuration (9·52, 6·36, 15·9) at $x/D = 14{\cdot}6$ was $(0{\cdot}98 + 0{\cdot}73)\,D = 1{\cdot}71D$, the half-wake widths of $0{\cdot}98D$ and $0{\cdot}73D$ referring to the portions of the wake downstream of the smaller and larger cylinders respectively. In this way it was possible to compare the growth of the wake generated by each cylinder separately.

Single hot-wire traverses were taken for the wakes at a range of streamwise locations. However, the main aim of the research was to find the characteristics at 14·6 and 80 diameters downstream, the latter being the limit of the test section. The longitudinal mean velocity and turbulent intensities in the x and y directions as well as the single-point correlation $\overline{vu}$ were measured. The lateral mean velocity, in the y direction, was very much smaller than other mean quantities, of the order of $0{\cdot}03U$ at most, and because of the large scatter, these results are not presented. Detailed measurements were made in the regions of production inequality to define the extent of the zone.

One-dimensional energy spectra for the $\overline{u^2}$, $\overline{v^2}$ and $\overline{uv}$ components were taken

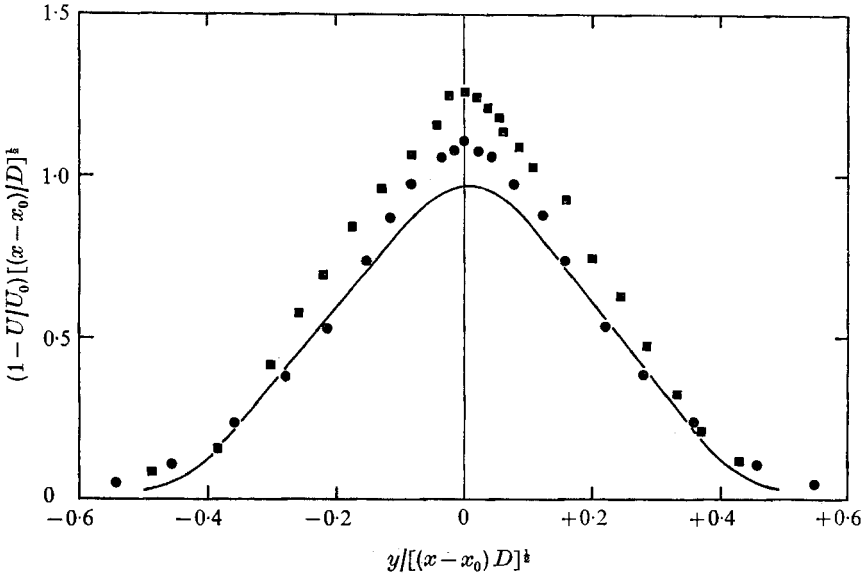

FIGURE 2. Mean velocity profiles for symmetric cylinder pair (12·7, 6·35, 12·7); ●, $x/D = 14{\cdot}6$; ■, $x/D = 80$; ——, single-cylinder wake data from Townsend (1956) for $x/D = 120$.

close to the cylinders to give some description of the complex vortex-shedding process. The $\overline{u^2}$ spectra were also measured at $x/D = 14{\cdot}6$ to evaluate turbulent integral scales and the dissipation in the presence of energy reversals.

3. Results

3.1. *Mean velocity*

The location of the maximum U velocity defect (U_m) was selected as the dividing streamline for the multiple wake flows. (The V component of the velocity was essentially zero over a wide range and its value could not be used as a criterion.) Figure 2 shows that the U profile for the symmetrical configuration matches closely the published single-cylinder results when scaled by the self-preserving transformations of Townsend (1956). In the asymmetrical situations, figures 3 (*a*), (*b*) and (*c*), profiles of U velocity at $x/D = 14{\cdot}6$ showed marked skewing towards the small-cylinder half of the wake. The skewing was still detectable at 80 diameters although tabulation of the third moments of area in table 1 for the mean velocity defect show this to have decreased significantly. (The small values of skewness listed for the symmetrical pair are a result of the numerical method used to evaluate the third moment.)

The half-wake widths are presented in table 1. For the asymmetrical combinations an interesting result emerges: the lateral extent of the defect zone was larger on the small-cylinder side of the wake. This is consistent with the results of Bragg & Suk (1972), who examined the flow downstream from a group of rods which were parallel but of unequal diameter. Again the spread of the turbulence was greater on the side with the small cylinders. A related feature has also been observed for basically different types of flows. Kuo & Baldwin (1967), who

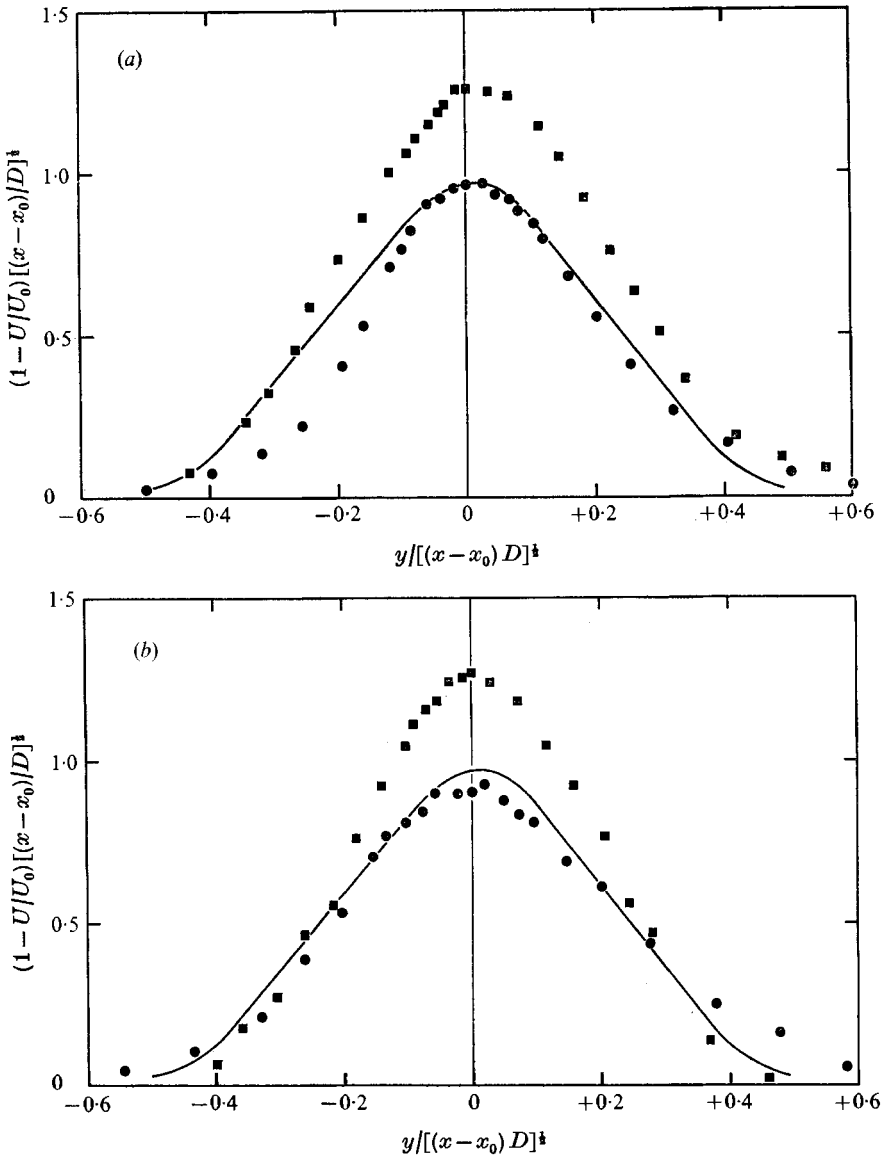

FIGURE 3(*a*, *b*). For legend see p. 599.

examined a three-dimensional elliptical wake, and Pratte & Keffer (1969), who studied a pair of swirling jets, noted a reversal in the rate of spread of the turbulent field, the maximum growth shifting from one principal axis to the other. In the present study, however, the half-wake width continued to be a maximum on the small-cylinder side up to the limit of observation, $x/D = 80$.

To explore the mean flow characteristics further an entrainment coefficient ψ was evaluated. For an axisymmetric flow, Morton (1961) defined ψ from the relation

$$\frac{d}{dx}\{\pi\rho r^2 U\} = 2\pi r\rho\psi|U - U_0|, \tag{3.1}$$

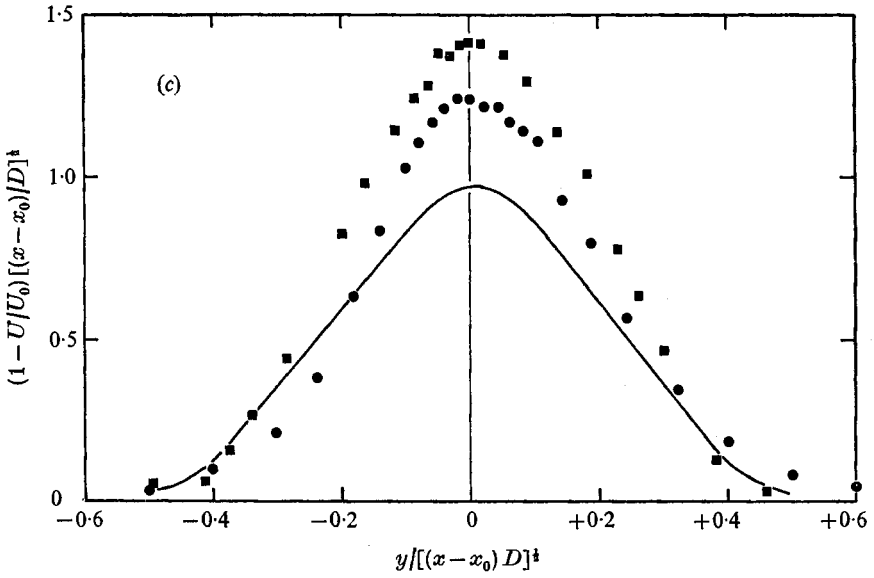

FIGURE 3. Mean velocity profiles for asymmetric cylinder pairs; ●, $x/D = 14{\cdot}6$; ■, $x/D = 80$; —, single-cylinder data, $x/D = 120$. (*a*) (12·7, 6·35, 15·9) pair; (*b*) (9·52, 4·78, 15·9) pair; (*c*) (9·52, 6·35, 15·9) pair.

Cylinder configuration	Total wake ψ	Small cylinder wake side ψ	Large cylinder wake side ψ	Ratio small-to-large
12·7, 6·35, 12·7	0·22	0·11	0·11	1·0
12·7, 6·35, 15·9	0·24	0·13	0·10	1·3
9·52, 4·79, 15·9	0·19	0·11	0·087	1·3
9·52, 6·35, 15·9	0·21	0·091	0·083	1·1
Single-cylinder two-dimensional wake after Ellison & Turner (1959)	0·22			

TABLE 2. Entrainment coefficients

where r is a characteristic radius for the developed flow, say the half-velocity point, U is the 'top-hat' value of velocity and U_0 is the free-stream velocity. We can adopt this expression for the present two-dimensional flow by considering a unit width of the wake (i.e. in the z direction). The expression becomes

$$\frac{d}{dx}\{\rho l_0 U_m\} = 2 l_0 \rho \psi (U_0 - U_m), \tag{3.2}$$

where U_m, the minimum velocity, has been used instead of an averaged defect term and l_0 is the half-velocity width of the wake. An estimate of ψ can be determined, using two streamwise stations x_1 and x_2, from

$$\rho l_0 U_m = 2\rho\psi[\tfrac{1}{2}(l_{0,1} + l_{0,2})]\,[U_0 - \{\tfrac{1}{2}(U_{m,1} + U_{m,2})\}]. \tag{3.3}$$

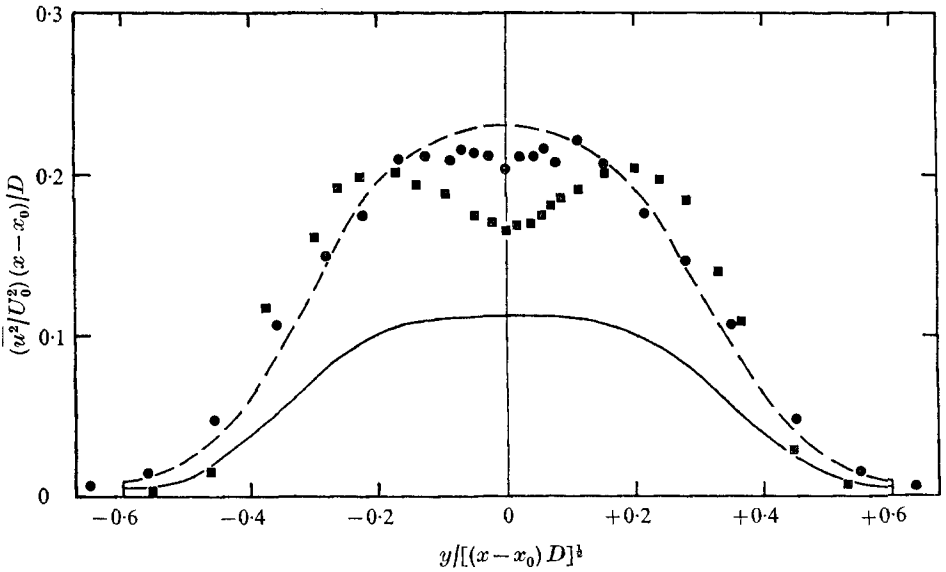

FIGURE 4. Streamwise turbulent intensities for symmetric cylinder pair (12·7, 6·35, 12·7); ●, $x/D = 14{\cdot}6$; ■, $x/D = 80$; – – –, single-cylinder data, $x/D = 80$; ——, single-cylinder data, $x/D = 120$.

The entrainment coefficients for all cylinder-pair configurations as well as that for a normal wake are listed in table 2. It is observed that the coefficients for the total wake of all twin-cylinder configurations are similar to that of a normal wake. However, the separate coefficients are larger on the small-cylinder half of the wake for the asymmetrical pairs, a consequence of the observed growth rate mentioned previously.

3.2. *Turbulent velocities*

Turbulent velocity profiles for $\overline{u^2}$, $\overline{v^2}$ and $\overline{uv}$ were measured at $x/D = 14{\cdot}6$ and 80. The results for $\overline{u^2}$ and $\overline{uv}$ are shown for the four configurations in figures 4–7. The $\overline{u^2}$ profile for the symmetrical twin-cylinder configuration (figure 4), in contrast to the mean velocity result, shows distinct departures from single-cylinder profiles. The individual contributions to the intensity level from each cylinder are reflected by the symmetrical peaks of the distribution. For the asymmetrical data, a maximum level of intensity occurs on the large-cylinder side of the flow although the double peak remains.

In contrast, the maximum absolute value of $\overline{uv}$ for the asymmetrical cases occurs on the small-cylinder portion of the wake. The high entrainment coefficients measured on this side are a direct consequence of an intense large eddy motion, the main mechanism for entrainment of free-stream fluid. The large-scale vorticity associated with this motion and the accompanying steep local levels of velocity gradients are consistent with the large values of Reynolds stresses measured behind the small cylinder. As expected, the $\overline{uv}$ profiles show no asymmetry for the symmetrical configuration.

It is extremely likely that the asymmetrical wake would eventually move

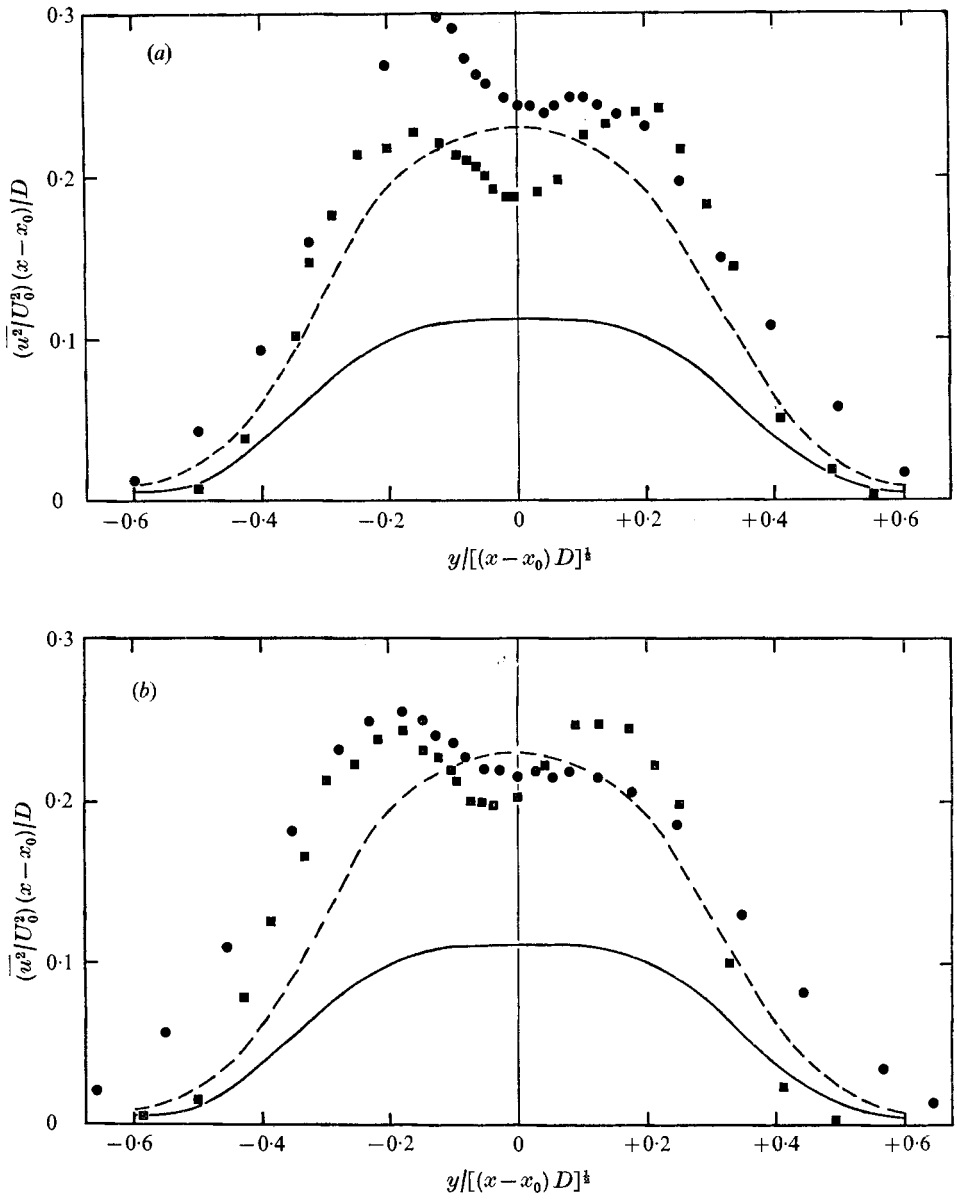

FIGURE 5(*a*, *b*). For legend see p. 602.

towards an equilibrium state in which the asymmetry would become negligibly small. Because of the rather intense vortical activity in the early period of the flow, one would expect this at very large distances downstream – perhaps only asymptotically. This does not seem to be the case, at least for the mean velocity. The asymmetrical mean velocity profiles show a rather rapid transition to normal wake values. However, within the limit of the test section the structure of the turbulent field appears to be evolving rather slowly.

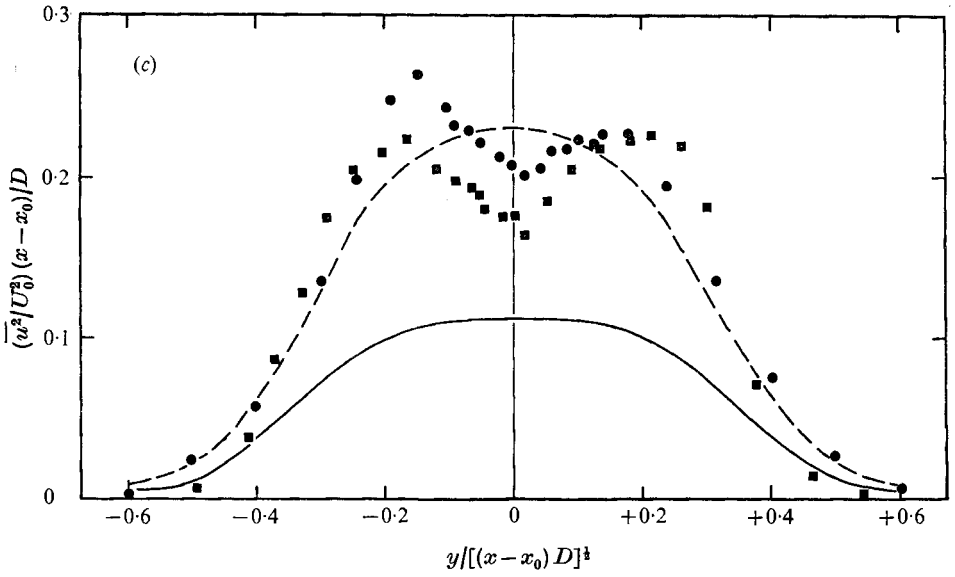

FIGURE 5. Streamwise turbulent intensities for asymmetric cylinder pairs; ●, $x/D = 14{\cdot}6$; ■, $x/D = 80$; – – –, single-cylinder data, $x/D = 80$; ——, single-cylinder data, $x/D = 120$. (*a*) (12·7, 6·35, 15·9) pair; (*b*) (9·52, 4·78, 15·9) pair; (*c*) (9·52, 6·35, 15·9) pair.

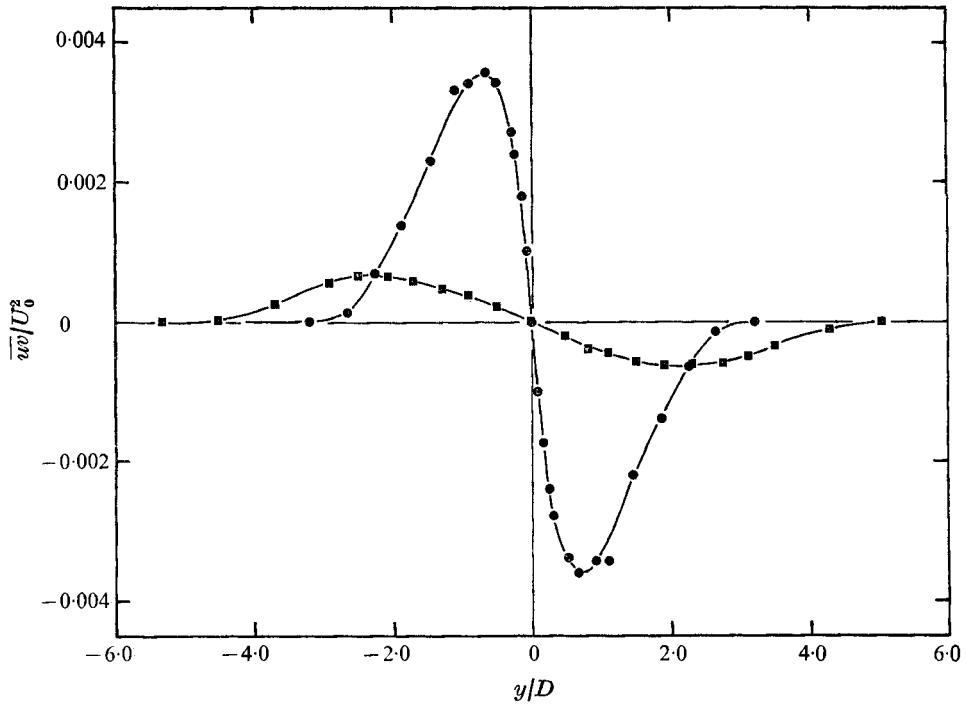

FIGURE 6. Reynolds shear stress for symmetric cylinder pair (12·7, 6·35, 12·7); ●, $x/D = 14{\cdot}6$; ■, $x/D = 80$.

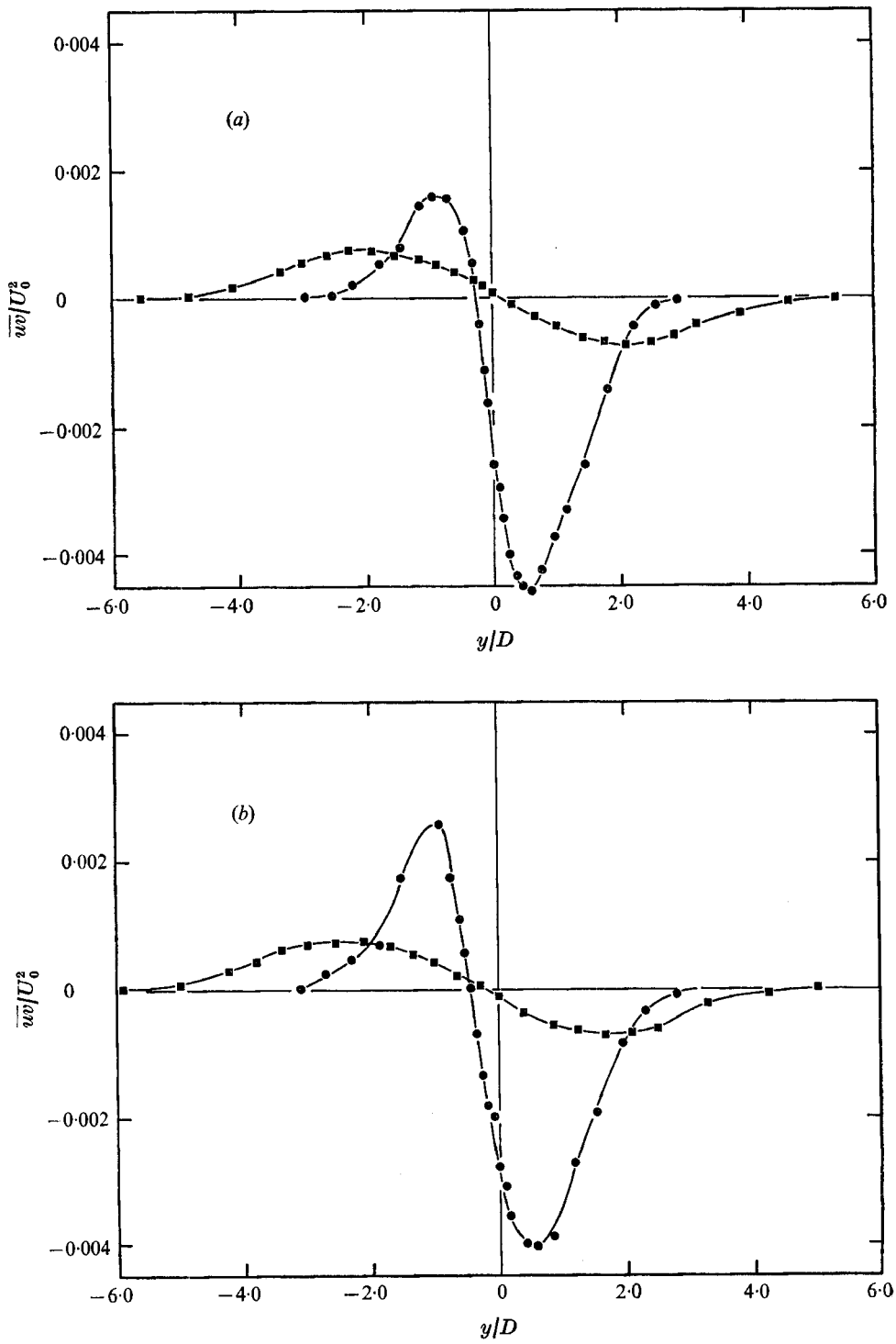

FIGURE 7 (*a*, *b*). For legend see p. 604.

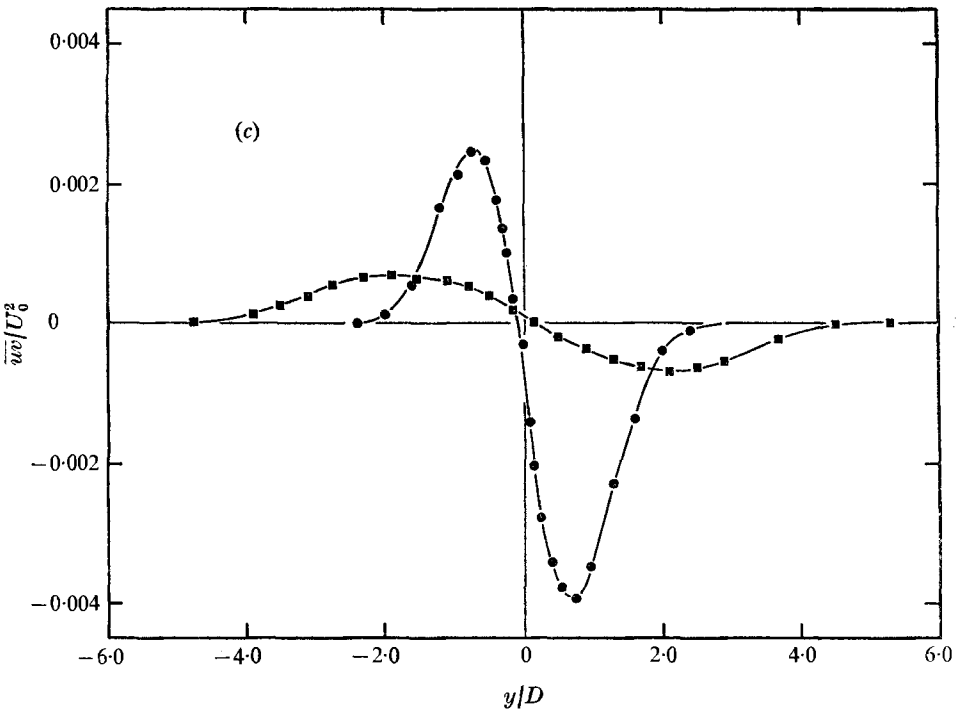

FIGURE 7. Reynolds shear stress for asymmetric cylinder pairs; ●, $x/D = 14{\cdot}6$; ■, $x/D = 80$. (*a*) (9·52, 6·35, 15·9) pair; (*b*) (9·52, 4·78, 15·9) pair; (*c*) (9·52, 6·35, 15·9) pair.

3.3. *Turbulent energy reversal*

It can be seen from the results for the asymmetrical cylinder pairs shown in figures 7 (*a*), (*b*) and (*c*) that the point of zero Reynolds stress does not coincide with the maximum velocity defect. We have described this situation as one of turbulent energy reversal and it is of interest to explore it in more detail.

Following Eskinazi & Erian (1969), we may integrate the turbulent kinetic energy equation over a representative volume α of the flow field:

$$\int_\alpha \frac{d}{dt}\left(\overline{\frac{q^2}{2}}\right) d\alpha = -\int_\alpha \frac{\partial}{\partial x_k}\left[\overline{u_i\left(\frac{p}{\rho}+\frac{q^2}{2}\right)}\right] d\alpha - \int_\alpha \overline{u_i u_k}\frac{\partial U_i}{\partial x_k} d\alpha$$

$$+\int_\alpha \nu \frac{\partial}{\partial x_k}\left[\overline{u_i\left(\frac{\partial u_i}{\partial x_k}+\frac{\partial u_k}{\partial x_i}\right)}\right] d\alpha - \int_\alpha \nu \overline{\frac{\partial u_i}{\partial x_k}\left(\frac{\partial u_i}{\partial x_k}+\frac{\partial u_k}{\partial x_i}\right)} d\alpha, \qquad (3.4)$$

where the terms have the conventional interpretation: the total rate of change of energy, diffusion by the turbulence, production of energy, diffusion by viscous action and finally, dissipation. The first and third terms on the right-hand side can be changed to surface integrals via the divergence theorem and if we assume that the flux across the boundaries is negligible the relationship simplifies to

$$\int_\alpha \frac{d}{dt}\left(\overline{\frac{q^2}{2}}\right) d\alpha = -\int_\alpha \overline{u_i u_k}\frac{\partial U_i}{\partial x_k} d\alpha - \int_\alpha \frac{\nu}{2}\overline{\left(\frac{\partial u_i}{\partial x_k}+\frac{\partial u_k}{\partial x_i}\right)^2} d\alpha, \qquad (3.5)$$

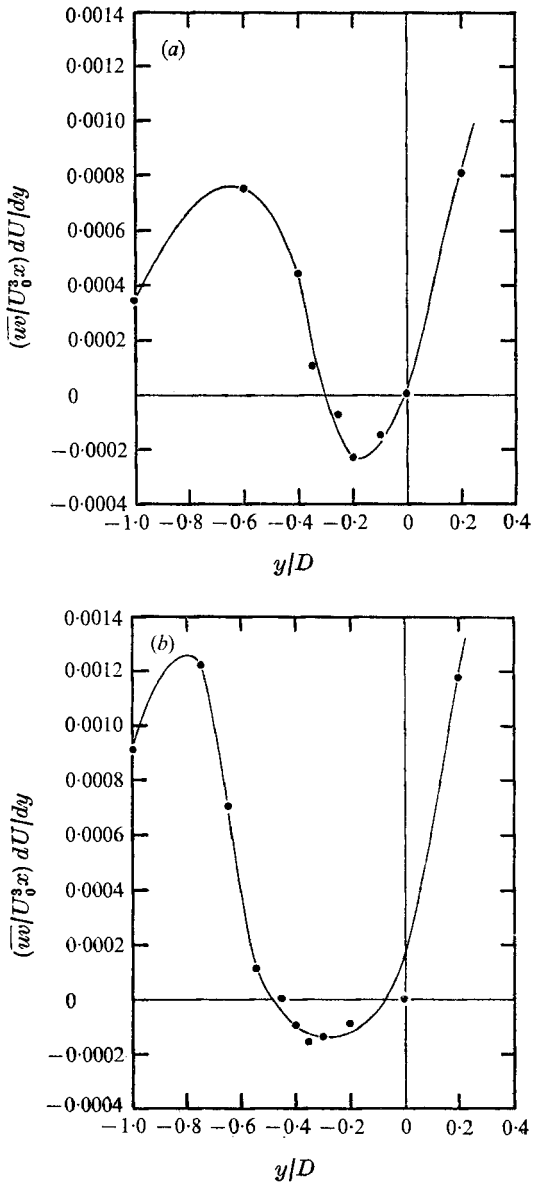

FIGURE 8 (*a*, *b*). For legend see p. 606.

the dissipation term being changed to a squared quantity. For a steady flow, the term on the left-hand side is zero, with the result that the production term is balanced by the dissipation. The latter is always positive and so we conclude that over the entire volume

$$-\int_{\alpha} \overline{u_i u_k} \frac{\partial U_i}{\partial x_k} d\alpha > 0. \tag{3.6}$$

However, for small enough regions of the flow the above restriction may not

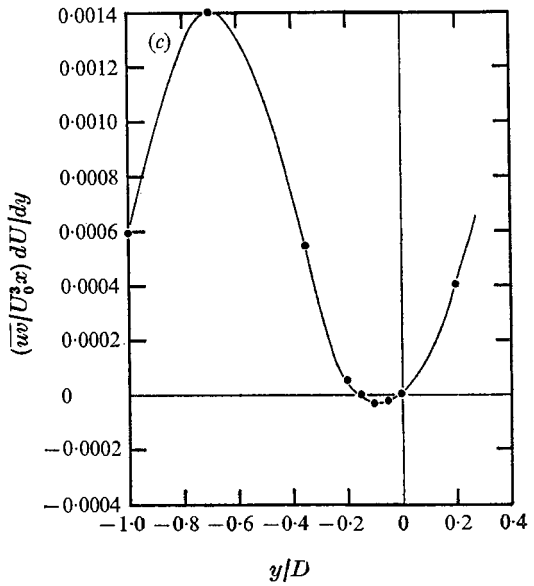

FIGURE 8. Energy reversal zone $x/D = 14{\cdot}6$. (*a*) (12·7, 6·35, 15·9); (*b*) (9·52, 4·78, 15·9); (*c*) (9·52, 6·35, 15·9).

hold. We can now expand the production term, which for a two-dimensional flow becomes

$$(\overline{u^2}-\overline{v^2})\frac{\partial U}{\partial x}+\overline{uv}\left(\frac{\partial V}{\partial x}+\frac{\partial U}{\partial y}\right). \tag{3.7}$$

In most turbulent shear flows the spread of the turbulence is moderate and it is permissible to invoke boundary-layer type approximations. Thus $\partial U/\partial y$ can be expected to be at least an order of magnitude greater than $\partial V/\partial x$. Furthermore, the turbulent intensities $\overline{u^2}$ and $\overline{v^2}$ will be of the same order. The present results support this and so the term $\overline{uv}\,\partial U/\partial y$ can be expected to control the local production in the multiple-wake flow. If, then, the signs of $\overline{uv}$ and $\partial U/\partial y$ differ in some part of the flow as indicated by the results in figure 4, we can conclude that an energy reversal exists over that region. The extent of the energy reversal regions for the present investigation are plotted in figures 8(*a*), (*b*) and (*c*).

3.4. *Energy spectra*

The one-dimensional energy spectrum function E_1 defined by

$$\int_0^\infty E_1(k)\,dk = \overline{u^2}, \tag{3.8}$$

where k = wavenumber $= 2\pi n/U$ and n = frequency in Hz, was measured in the region of energy reversals. It was assumed that the flow was locally isotropic in the high wavenumber region of the spectra so that an estimate of the dissipation ϵ and a form of integral scale Λ of the flow could be obtained from

$$\epsilon = 15\nu\int_0^\infty k^2 E_1(k,t)\,dk, \tag{3.9}$$

$$\Lambda = \frac{\pi}{2\overline{u^2}}\int_0^\infty \frac{E_1(k,t)}{k}\,dk. \tag{3.10}$$

Cylinder configuration	Wake		Energy reversal region		
	$\frac{\epsilon x}{U_0^3} \times 10^3$	$\frac{\Lambda}{[(x-x_0)D]^{\frac{1}{2}}}$	$\frac{\epsilon x}{U_0^3} \times 10^3$	$\frac{\Lambda}{[(x-x_0)D]^{\frac{1}{2}}}$	$\frac{1}{U_0^3}\frac{d}{dy}\left(\frac{\overline{vq^2}}{2}\right) x \times 10^5$‡
12·7, 6·35, 12·7	4·4	0·29			6·6
12·7, 6·35, 15·9	3·3†	0·49†	4·5	0·22	8·7
9·52, 4·78, 15·9	3·0†	0·49†	4·2	0·28	8·0
9·52, 6·35, 15·9	2·9†	0·36†	3·5	0·25	10·6
Normal wake (Portfors 1969)	5·0	—	—	—	—

† For asymmetrical case, these terms were determined on the small diameter portion of the wake where no energy reversal existed.

‡ Estimated from $\frac{d}{dy}\left[\frac{(\overline{v^2})^{\frac{1}{2}}\overline{q^2}}{2}\right]$.

TABLE 3. Turbulent dissipation and integral scales at $x/D = 14{\cdot}6$

The experimental results are presented in table 3. Both dissipation and integral scales for the symmetrical twin-cylinder configuration are similar in magnitude to normal-wake data. However, for the asymmetrical cylinder configurations the integral scales are greater on the small-cylinder half of the wake, where the entrainment is the largest. The opposite is true for the dissipation measurements, which are higher in the region of the energy reversal. The maximum turbulent diffusion was also estimated from the results and is compared in table 3. It was found to be a maximum in the region of the reversal, which agrees with the results of both Béguier (1965) and Eskinazi & Erian (1969).

3.5. *Vortex shedding*

With the larger entrainment coefficients, for which larger values of integral scales and Reynolds stress appear on the small-cylinder half of the wake, one expects a well-defined but asymmetric vortex-shedding mechanism to exist. This proved to be the case. The vortices remained persistent and easily identifiable as separate structures well downstream of the cylinders and were readily observed on visicorder and oscilloscope traces made with the hot-wire anemometer. A typical example of the measured energy spectra is presented in figure 9. Both the fundamental vortex-shedding frequency and its harmonics are apparent.

The flow visualization experiments revealed the existence of a large attached eddy at the rear of the large-diameter cylinder. The low pressure associated with the attached eddy and the accelerated flow through the gap between the cylinders appeared to assist the formation of the strong vortex pattern described above. As observed earlier, the mean velocity defect was significantly skewed towards the small-cylinder portion of the wake, which suggests that the mean flow drag was greater behind the smaller cylinder. This aspect was not pursued further here.

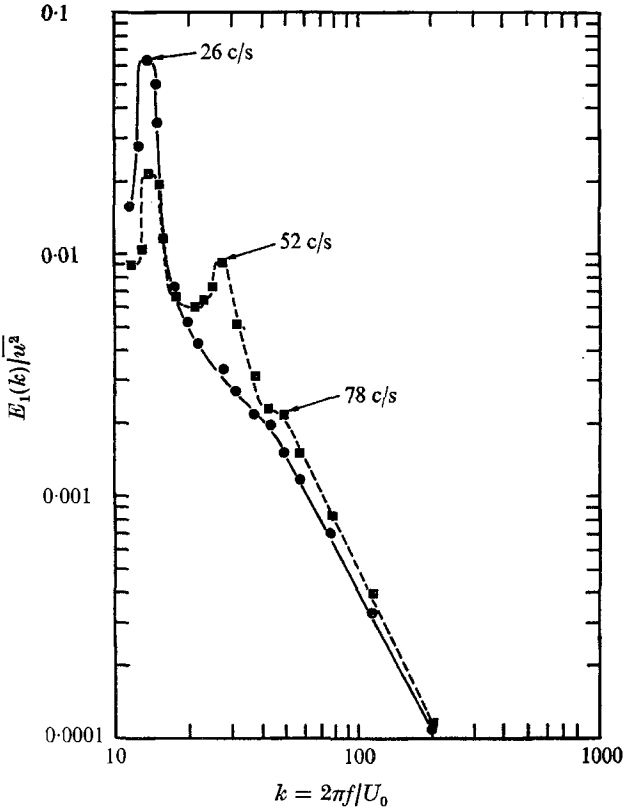

FIGURE 9. One-dimensional energy spectra for streamwise turbulent intensity component; asymmetrical cylinder pair (9·52, 6·35, 15·9); $x/D = 3{\cdot}3$; ●, $y/D = +0{\cdot}1$; ■, $y/D = -0{\cdot}3$.

4. Discussion

The transformed mean velocity profiles were nearly symmetrical at 80 diameters downstream for all cylinder configurations and similar in shape to the normal-wake data. However, a negative shift of the virtual origin was required to match the results with the single-cylinder wake data. This suggests a more rapid streamwise flow development for the combined flow, which is rather surprising. One would expect that the introduced asymmetry would delay the approach of the flow to an equilibrium state. It appears, however, that the strong vortex pattern generated in the asymmetrical cases provides an effective transport mechanism across the wake and increases mixing within the wake. This behaviour is confirmed by examining the entrainment coefficients (table 2) and integral scales (table 3). Both of these were larger for the asymmetrical cases downstream of the smaller cylinder.

For the symmetrical flow the results for the turbulent intensities $\overline{u^2}$ and $\overline{v^2}$ exhibited a double-peak profile at $x/D = 80$, an effective shadow from the cylinder configuration. There was no corresponding behaviour for the mean velocity profiles, which is not surprising; mean velocities are characteristically less sensitive measures of self-similarity than the turbulent quantities.

One would assume that the most probable form for this complex turbulent wake would be symmetrical, and the present asymmetrical behaviour could be considered merely a strong perturbation upon the initial conditions of the system. From the above comments it would seem that this perturbation has the effect of driving the flow towards its asymptotic form prematurely. There is a precedent for this reasoning. Portfors (1969) found that the generation of grid flow turbulence using a series of parallel rods, which were aligned in the z direction, created strong peaks in the energy spectra of the $\overline{u^2}$ and $\overline{v^2}$ components, but not the $\overline{w^2}$ components. (Such asymmetrical peaks do not appear for bi-plane grid flows.) In Portfors's case, the peaks were at least an order of magnitude above the general energy level with the result that both intercomponent energy transfer (to $\overline{v^2}$) and the cascade of kinetic energy down the spectra were enhanced. It was found that after 40 grid spacings downstream the flow was essentially isotropic in terms of both intensity components and spectra. A similar peaking occurs in the intensity of turbulence and energy spectra for the twin-cylinder configurations examined here.

It is quite possible that a threshold value of asymmetry might be required for energy reversal to occur. The results show that turbulent diffusion, the major mechanism available in the flow for redistributing energy, reaches a maximum in the zone of energy reversal. Evidently, the wake must attempt to redistribute the turbulent energy by diffusing and transporting (by large eddies) the turbulent energy to regions of increased turbulent dissipation downstream of the smaller cylinder. When these mechanisms are not sufficiently large to handle the excess turbulence produced by the cylinder geometry, a local energy reversal takes place and it is this mechanism which re-establishes an equilibrium.

It has been suggested by Deissler (1968) that the corresponding phenomena observed in meteorological situations are a result of a rapid change in the decay rate of turbulence. This particular aspect was not investigated in our experiment but, in a sense, the two mechanisms are connected. If the local energy equilibrium is destabilized by a sudden increase in the rate of dissipation (or perhaps by a decrease in the spectral transfer of energy to higher wavenumbers) the energy content in the production range of the spectrum must increase. A possible consequence would be a local reversal of the energy to small wavenumbers. In our present situation, no destabilizing occurs but an excessive quantity of turbulent energy, caused by the particularly strong asymmetry of the wake generators, has a similar effect. The diffusive and convective mechanisms cannot establish an equilibrium, and the excessive kinetic energy appears in the lower wavenumbers. Clearly, the magnitude of the asymmetry must be a controlling factor. Slightly asymmetrical flow fields may not generate measurable reversals.

This work was carried out under National Research Council of Canada Grant A-2746. One of the authors (M.D.P.) was supported during the course of the research by a McAllister Fellowship, which is gratefully acknowledged. We would like to thank Richard Blumenauer for his assistance in taking some of the data.

REFERENCES

ALEXOPOULOS, C. C. & KEFFER, J. F. 1968 Extended measurements of the two-dimensional turbulent wake. *Dept. Mech. Engng., University of Toronto, Tech. Publ. Ser.* UT MECH E TP6811.

BÉGUIER, C. 1965 Mesures des tensions de Reynolds dans un encoulement dissymetrique en régime turbulent incompressible. *J. Mécanique*, **4**, 319.

BLOOR, M. S. 1964 The transition to turbulence in the wake of a circular cylinder. *J. Fluid Mech.* **19**, 290.

BRAGG, G. M. & SUK, J. K. 1972 Arbitrary mean flow in adverse pressure gradients. *J. Bas. Engng. Trans. A.S.M.E.* D **93**, 495.

DEISSLER, R. G. 1968 Production of negative eddy conductivities and viscosities in the presence of buoyancy and shear. *Phys. Fluids*, **11**, 432.

ELLISON, T. H. & TURNER, J. S. 1959 Turbulent entrainment in stratified flows. *J. Fluid Mech.* **6**, 432.

ESKINAZI, S. & ERIAN, F. F. 1969 Energy reversal in turbulent flows. *Phys. Fluids*, **12**, 1988.

GERRARD, J. H. 1965 A disturbance-sensitive Reynolds number range of flow past a circular cylinder. *J. Fluid Mech.* **22**, 187.

HAMA, F. R. 1962 Progressive deformation of a curved vortex filament by its own induction. *Phys. Fluids*, **5**, 1156.

KRUKA, V. & ESKINAZI, S. 1964 The wall jet in a moving stream. *J. Fluid Mech.* **20**, 555–579.

KUETHE, A. M. 1951 Some aspects of boundary-layer transition and flow separation on a cylinder in yaw. *1st Midwestern Conf. on Fluid Mech.* p. 44.

KUO, Y.-H. & BALDWIN, L. V. 1967 The formation of elliptical wakes. *J. Fluid Mech.* **27**, 353.

LUMLEY, J. L. & PANOFSKY, H. A. 1964 *The Structure of Atmospheric Turbulence.* Interscience.

MORTON, B. R. 1961 On a momentum mass flux diagram for turbulent jets, plumes and wakes. *J. Fluid Mech.* **10**, 101.

PORTFORS, E. 1969 Isotropy in strained and unstrained turbulence. Ph.D. thesis, University of Toronto.

PRATTE, B. D. & KEFFER, J. F. 1969 Swirling turbulent jet flows. Part 2: the counter rotating jet pair. *Depth. Mech. Engng, University of Toronto, Tech. Publ. Ser.* UT MECH E TP6906.

SCHLICHTING, H. 1968 *Boundary-Layer Theory.* McGraw-Hill.

SPIVACK, H. M. 1946 Vortex frequency and flow pattern in the wake of two parallel cylinders at varied spacing normal to an air stream. *J. Aero. Sci.* **13**, 289.

TOWNSEND, A. A. 1956 *The Structure of Turbulent Shear Flow.* Cambridge University Press.

WONG, E. Y. J. & BRUNDIDGE, K. C. 1966 Vertical and temporal distributions of the heat conductivity and flux. *J. Atmos. Sci.* **23**, 167.